A Novel EOS That Combines van der Waals and Dieterici Potentials

Ilya Polishuk and Juan H. Vera
Dept. of Chemical Engineering, McGill University, Montreal, Quebec, Canada H3A 2B2

DOI 10.1002/aic.10441
Published online May 16, 2005 in Wiley InterScience (www.interscience.wiley.com).

A novel approach is proposed for solving the problem of the overestimation of the liquid–liquid equilibrium (LLE) range in mixtures typically associated with the use of equations of state (EOS) of the van der Waals type. This approach modifies the internal EOS structure by combining the van der Waals and the Dieterici forms. It advantageously uses the drawback of the Dieterici form, which strongly underestimates the LLE range. Thus, the new EOS is capable of generating an appropriate balance for the representation of vapor–liquid equilibria (VLE) and LLE critical data and therefore represents a major improvement in comparison with typical van der Waals–type EOSs. In addition, it gives accurate representation of the Joule–Thomson inversion curve and predicts critical data for nonpolar mixtures without any binary parameters. For polar systems, the novel EOS predicts critical data for complete homologous series of mixtures using a pair of binary parameters evaluated from a single system. © 2005 American Institute of Chemical Engineers
AIChE J, 51: 2077–2088, 2005
Keywords: thermodynamics/classical; phase equilibrium; mathematical modeling; hydrocarbon processing; supercritical processes

Introduction

A well-known problem associated with the use of equations of state (EOSs) for representing mixture data is their inability to establish a proper balance between the description of the vapor–liquid equilibrium (VLE) and the liquid–liquid equilibrum (LLE) data. In particular, a typical drawback of conventional van der Waals–type EOSs is their tendency to overestimate the range of liquid–liquid immiscibility. This feature limits the ability of the EOS to correlate both the VLE and LLE for the same system using a single set of binary adjustable parameters. A solution to this problem was obtained by introducing a temperature dependency for the binary cohesive energy adjustable parameter (Polishuk et al., 2003). Such temperature dependencies generate larger values of the binary parameter in the high-temperature VLE range and smaller values in the low-temperature LLE range. A similar temperature dependency is also introduced by the Huron–Vidal type G^E-based mixing rules (Huron and Vidal, 1979), and this explains their partial success over the classical quadratic mixing rules used in EOSs (Polishuk et al., 2002).

The introduction of an additional empirical temperature dependency into binary parameters of EOS models may fit the purpose but it does not contribute to their robustness and reliability. However, the possibility of improving the balance between the VLE and LLE representation by EOS models by modifying their internal structure, instead of introducing corrections to the binary parameters, has not received proper attention. In a recent publication (Polishuk et al., 2000) it was demonstrated that replacement of the van der Waals repulsive term, by the form proposed by Carnahan and Starling (1969), affects the balance between the VLE and the LLE by increasing the LLE range. Analytical EOS models used for quantitative representation of experimental data are combinations of theoretically based analytical forms and empirical terms. Their success is mostly attributed to the establishment of an appro-

Permanent address of I. Polishuk: Dept. of Chemical Engineering and Biotechnology, The College of Judea and Samaria, Ariel, Israel; e-mail: polishyk@bgumail.bgu.ac.il.
Correspondence concerning this article should be addressed to J. H. Vera at juan.vera@mcgill.ca.

priate cancellation of errors than to their rigorous theoretical base. Thus, the possibility of further improvement of the present van der Waals–type of EOS seems limited and it is desirable to explore novel alternative approaches.

Sadus (2001, 2002, 2003) recently revisited the rarely used approach of Dieterici, which presents an interesting alternative to the traditional van der Waals EOS structure. A global analysis of the Dieterici EOS was later presented by Bumba and Kolafa (2004) and by Polishuk et al. (2005). In the work of Polishuk et al. (2005) it was demonstrated that the fact that Dieterici EOS isotherms do not cross the zero-pressure axis to give negative pressures limits the possibility of this EOS to generate transitional mechanisms with negative pressure critical lines. This limitation has the potential to produce wrong predictions for the temperature dependency of the surface tension and it hinders the representation of the liquid–liquid immiscibility (Polishuk et al., 2005). Thus, although the typical structure of van der Waals EOS tends to overestimate the LLE range, the alternative structure of the Dieterici EOS leads to an underestimation of LLE. This observation suggests the possibility of achieving an appropriate balance between VLE and LLE by *combining both approaches into one EOS*. In what follows we discuss the implementation of this idea.

Theory

In contrast to the structure of van der Waals EOSs, which takes the difference between a term representing the repulsive forces and a term representing attractive forces, the Dieterici EOS presents a multiplication of these terms

$$P = \frac{RT}{v-b}\exp\left(-\frac{a}{RTv}\right) \tag{1}$$

where the first factor on the right-hand side is the van der Waals term used to represent repulsive forces and the exponential term contains the typical van der Waals parameter representing the cohesive forces. Expanding the exponential term in Eq. 1, and truncating the expansion after the second term, at low densities, Eq. 1 gives

$$P \approx \frac{RT}{v-b}\left(1-\frac{a}{RTv}\right) = \frac{RT}{v-b} - \frac{a}{v(v-b)} \tag{2}$$

This form more adequately shows the analogy between the approaches of Dieterici and van der Waals. In Eq. 1, the constants a and b are obtained from the ordinary stability mechanical conditions at the critical point (Polishuk et al., 2005). The fact that the constants a and b of the Dieterici EOS are similar to the values typically obtained by EOSs of the van der Waals type suggests the idea of combining both approaches into one single engineering EOS model, which could simultaneously yield an appropriate presentation of liquid densities and vapor pressures. From a theoretical perspective such a combination can be justified by considering the basic molecular assumptions used by the van der Waals and the Dieterici equations. In the van der Waals approximation, the pressure exerted over the wall of a vessel containing a system of hard bodies is given by the term $RT/(v-b)$. Because of the cohesive forces between molecules, a real fluid will exert a pressure over the walls lower than that of a system of hard bodies at the same temperature and molar density. Thus, the van der Waals model introduced a correction in the form of an average cohesive energy term that is subtracted from the hard body pressure. On the other hand, Dieterici's approach considers that only some molecules with enough kinetic energy would escape the cohesive energy field of the fluid to exert pressure over the walls of the container, giving the form of Eq. 1. Although both effects are interdependent for the same real fluid, they are not mutually exclusive. Thus, we incorporate both corrections to the hard body pressure as follows

$$P = \frac{RT}{v-b}\exp\left(-\frac{Wa}{RTv}\right) - \frac{a}{(v+c)(v+d)} \tag{3}$$

where W is a weighing factor. For a value zero of the weighing factor, $W = 0$, the typical four-parameter van der Waals form is recovered. Increasing the numerical value of the factor W increases the numerical contribution of the Dieterici part of the attractive term and it could be expected to decrease the van der Waals overprediction of liquid–liquid separation. The imperfect ability of EOS models to predict vapor pressures is corrected attaching the parameter a by empirical temperature dependencies (Anderko, 2003; Valderrama, 2003). Following previous studies of the van der Waals model (Polishuk et al., 2003), we use

$$a = a_c\alpha \tag{4}$$

where a_c is the value of the parameter at the critical temperature. In Eq. 4, the function α is given by

$$\alpha = T_r^{(m_1 T_r^{m_2})} \tag{5}$$

where T_r is the reduced temperature and m_1 and m_2 are adjustable parameters obtained from the fitting of the vapor pressure curve for the pure compound. Following the method previously used to evaluate four pure compound parameters for the van der Waals form (Polishuk et al., 2003), the parameter b is set equal to the liquid molar volume at the triple point, and the calculated critical volume is set at its experimental value multiplied by dimensionless volume shift whose numerical value is equal to $(1 + b)$. Thus, the parameters a_c, c, and d are evaluated by solving the system of three equations obtained from setting equal to zero the first two derivatives of the pressure with respect to the volume at the critical point and the condition for the EOS critical volume (Polishuk et al., 2003).

As shown in Table 1, the values of the pure compound parameters a_c, c, and d depend on the value of the scaling factor W. An increase in the value of W causes the values of volumetric parameters c and d to approach each other until they become identical. Thus, for each pure compound there is a limiting maximum value of the factor W at which the conditions given for parameters of Eq. 3 can be satisfied. On the other hand, as depicted in Figure 1, an increase of the value of W increases the minimal pressure reached by isotherms. Thus, the question is to what degree of negativity the isotherms should be to give a proper representation of the transitional mechanisms with negative pressure critical lines. Unfortu-

Table 1. Values of Parameters in Eqs. 3 and 5

Compound	W	a bar mol^{-1} L^{-1}	b (L/mol)	c (L/mol)	d (L/mol)	m_1	m_2
CH_4	0	2.86504	0.03549	−0.02929	0.10300	−0.15398	−0.33244
	1/5	2.38718	0.03549	−0.01640	0.11041	−0.20414	−0.18719
	0.57947 maximum	1.69423	0.03549	0.04022	0.04022	−0.33394	−0.60593
n-C_5O_{12}	0	22.1770	0.09548	−0.06290	0.29513	−0.59724	0.28539
	1/5	17.9142	0.09548	0.01868	0.22602	−0.60982	0.13494
	0.27415 maximum	16.5752	0.09548	0.11597	0.11597	−0.65744	0.19197

nately, this question does not have a definite answer that can be supported by experimental data. On the other hand, we can certainly evaluate whether the numerical contribution of the Dieterici part in Eq. 3 improves the ability of this model to describe some known experimental facts.

One of the best criteria to test the robustness and reliability of an EOS model for predicting different thermodynamic properties, over a wide range of temperatures and pressures, is its ability to describe the Joule–Thomson inversion curve (Wisniak and Avraham, 1996). This is explained by the fact that the accuracy in predicting this inversion curve is related to the ability of the model to simultaneously predict the volumetric and calorimetric properties. Figure 2 depicts an example of the influence of an increase in the value of the factor W in the prediction of the Joule–Thomson inversion curve for methane. It is seen that the value zero for this factor, which reduces Eq. 3 to the ordinary van der Waals form, leads to underestimation of the maximum inversion pressure. The contribution of the Dieterici part in Eq. 3 obtained by increasing the numerical value of W improves the results, and these become optimal at around the maximum limiting value of W. Such a result can be expected considering that the original EOS of Dieterici overestimates the Joule–Thomson inversion data (Polishuk et al., 2005). For comparison, in Figure 2 we have included the predictions obtained with the Peng–Robinson (PR) EOS (Peng and Robinson, 1976), the EOS of Redlich–Kwong (RK) (Redlich and Kwong, 1949) implemented with the Twu temperature dependency for the cohesive parameter or RK–Twu model (Twu et al., 1995, 1996) and the Dieterici–Carnahan–Starling (DCS) EOS, recently proposed by Sadus (2003).

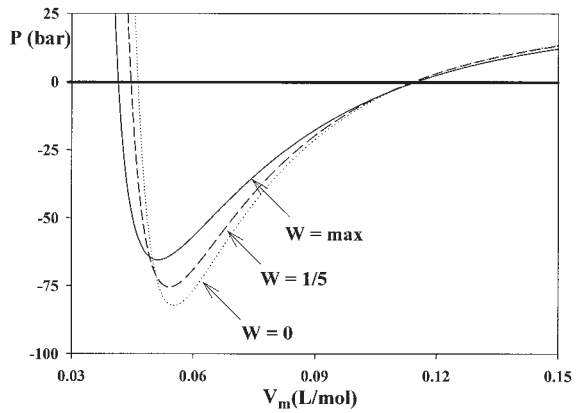

Figure 1. Isotherm T_r = 0.8 of methane predicted by Eq. 3 with different values of W.

Dotted line: W = 0; dashed line: W = 1/5; solid line: W = max.

Maxwell's equations indicate that different thermodynamic properties are interrelated. Therefore it is expected that the accuracy with which equations of state can predict the maximum Joule–Thomson inversion pressure would be related to the accuracy in predicting the critical pressure maximum (CPM) for *nonpolar* mixtures. In this work we use the following classical mixing rules

$$p = \sum_{ij} x_i x_j p_{ij} \tag{6}$$

where $p = a$, Wa, b, c, or d. The cross-interaction parameters are obtained using the following combination rules

$$p_{ij} = p_{ji} = \sqrt{p_{ii} p_{jj}} \tag{7}$$

for $a = a_c\alpha$ and for Wa. For b, c, or d we use

$$p_{ij} = p_{ji} = \frac{p_{ii} + p_{jj}}{2} \tag{8}$$

Figure 3 illustrates the predictive performance of the critical pressure maximum for the methane–*n*-pentane system. The larger overestimation of the critical data is given by the DCS EOS, which is directly related to the overprediction of the Joule–Thomson inversion curve by this model. Notably, the

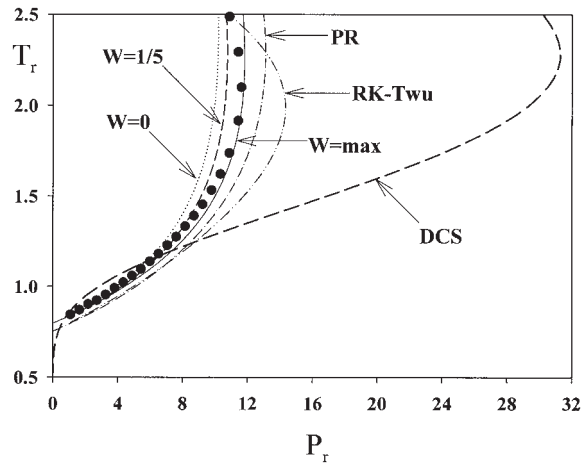

Figure 2. Joule–Thomson inversion curve of methane.

●: Experimental data of Perry et al. (1999); dotted line: W = 0; dashed line: W = 1/5; solid line: W = max; dot–dashed line: EOS of Peng and Robinson (1976); dot–dot–dashed line RK–Twu EOS; thick dotted line: DCS EOS.

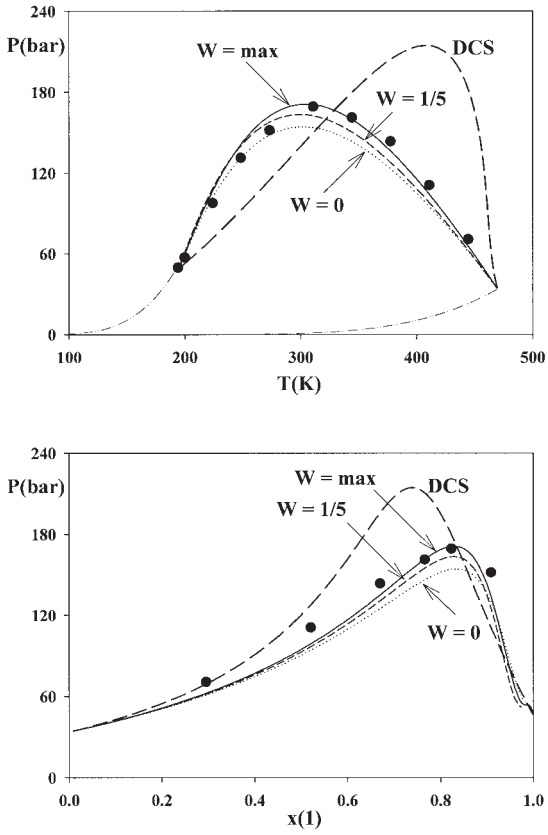

Figure 3. Critical data of methane(1)–*n*-pentane(2).

●: Experimental data of Chen et al. (1978) and Sage et al. (1942); dotted line: $W = 0$; dashed line: $W = 1/5$; solid line: W = max; thick dotted line: DCS EOS; dot–dot–dashed line: vapor pressure line.

Joule–Thomson inversion curve given by the DCS EOS goes to pressures even higher than those obtained with the original Dieterici EOS. This observation may explain the recent results of Sadus (2003), who obtained higher critical pressures from the DCS EOS than from the original Dieterici EOS.

Because—similarly to the Dieterici EOS—the DCS EOS does not generate negative pressures, it is to be expected that the DCS EOS will fail to describe the experimentally observed transitions between types of phase behavior and will underestimate the range of LLE (Polishuk et al., 2005). As a result it is not expected that this EOS will be able to simultaneously fit VLE and LLE data. The introduction of a temperature functionality in the DCS EOS will not solve its fundamental structural disadvantages. Therefore we will not include this EOS in further comparisons.

Notably, Eq. 3 also presents the same regularity in performance with different values of W, as found in Figure 2. It can be seen that in the absence of the Dieterici part ($W = 0$) the model underpredicts not only the maximum inversion pressure of methane, but also the CPM of the methane–*n*-pentane system, using Eqs. 6–8. However, the introduction of the Dieterici part into Eq. 3 ($W \neq 0$) improves not only the results for the Joule–Thomson inversion, but also of the CPM, which, again, becomes exact at the maximum limiting value of the weighting parameter W.

The CPM is a key point for the description of mixture phase diagrams because it characterizes the extension of the VLE region in the system. Thus, an inability to predict the exact value of CPM results in an inaccurate description of VLE phase boundaries. Usually, for the case of two pure compound parameters, this problem has been solved by introduction of two binary adjustable parameters k_{12} and l_{12} into Eqs. 7 and 8 as follows

$$p_{ij} = p_{ji} = (1 - k_{ij}) \sqrt{p_{ii} p_{jj}} \tag{9}$$

for a and Wa. For b we use

$$b_{ij} = b_{ji} = (1 - l_{ij}) \frac{b_{ii} + b_{jj}}{2} \tag{10}$$

For c and d Eq. 8 is used. In the case of the Peng–Robinson (PR) EOS (Peng and Robinson, 1976), the predictions without binary parameters overestimate the CPM data using Eqs. 7 and 8, and there is a need to introduce a negative value of k_{12} (Polishuk et al. 1999) to correlate the data. As shown in Figure 2, this EOS also overestimates the maximum pressure of the Joule–Thomson inversion curve.

In contrast, Eq. 3—with an insufficient contribution of the Dieterici part ($W = 0$ and $W = 1/5$)—underestimates both the Joule–Thomson and the CPM data and would require a positive value of k_{12} for an appropriate description of the data of the methane–*n*-pentane system. However the results achieved by adjusting only one binary parameter are not satisfactory, given that both the PR EOS and Eq. 3, with low values of W, fail to predict the experimentally measured continuous critical line of Type I for the system under consideration. Again, this result is explained by the fact that van der Waals–like EOSs tend to overestimate the range of LLE and for this reason they tend to predict a liquid–liquid split for many systems that do not exhibit it in practice. Thus, to generate an appropriate description of a binary phase diagram there is a need to introduce the second adjustable parameter l_{12} (Polishuk et al., 2003). The need to fit adjustable parameters to data for each particular binary system is a major drawback because it takes away the predictive properties of the model.

In this respect the results presented by Eq. 3 with the maximum limiting value for W are promising. This model not only has a clear superiority in prediction of the Joule–Thomson inversion curve and the CPM, but also has a better ability to predict the correct topology of phase behavior. It is evident that the introduction of the Dieterici part into the EOS reduces the range of liquid–liquid immiscibility generated by the EOS model and thus improves the overall performance of the model. Second, these results indicate a possibility of implementing the model under consideration for predicting the data in nonpolar mixtures *without a need to adjust the binary parameter*s. At the maximum value of W, Eq. 3 takes the following form

$$P = \frac{RT}{v - b} \exp\left(-\frac{Wa}{RTv}\right) - \frac{a}{(v + c)^2} \tag{11}$$

In some sense, the factor W becomes a fourth parameter and its value is fixed by the condition $c = d$. Values of parameters for

Table 2. Values of Parameters in Eq. 11

Compound	a bar mol^{-1} L^{-1}	b (L/mol)	c (L/mol)	W	m_1	m_2
Hydrogen	0.17840	0.02331	0.02078	0.56974	−0.05610	0.10016
Nitrogen	1.01339	0.03221	0.03355	0.55153	−0.40072	−0.14596
Carbon dioxide	2.34564	0.03728	0.05259	0.90275	−0.63613	−0.98491
Methane	1.69423	0.03549	0.04022	0.57947	−0.33394	−0.60593
Ethane	4.61708	0.04621	0.05670	0.36672	−0.44921	0.06051
Propane	8.08217	0.06030	0.07420	0.29191	−0.51466	0.10006
n-Butane	11.9028	0.07924	0.09291	0.29447	−0.60520	0.28434
n-Pentane	16.5752	0.09548	0.11597	0.27415	−0.65744	0.19197
n-Hexane	21.7672	0.11433	0.13396	0.25312	−0.76381	0.37736
n-Heptane	27.5435	0.12987	0.15742	0.23352	−0.75271	0.09011
n-Octane	33.5550	0.15025	0.18407	0.23654	−0.81529	0.09982
n-Nonane	40.2723	0.16647	0.20760	0.21948	−0.86466	0.11736
n-Decane	48.7110	0.18584	0.19624	0.14791	−0.98029	0.28131
n-Dodecane	62.6747	0.22157	0.29542	0.20577	−0.97307	0.01391
n-Tetradecane	80.8668	0.25691	0.38778	0.21070	−1.03005	−0.00942
n-Hexadecane	99.5104	0.29251	0.44879	0.19518	−0.96587	−0.19039
n-Eicosane	138.169	0.36369	0.52377	0.14882	−1.38740	0.17468
Methanol	8.50017	0.03583	0.09858	0.40370	−0.87673	−0.57270
Ethanol	10.7736	0.05151	0.11204	0.40792	−0.91714	−0.73524
2-Propanol	13.4558	0.06823	0.12689	0.38517	−0.95194	−0.56035
n-Propanol	14.5351	0.06525	0.12900	0.35916	−0.78672	−0.90548
2-Butanol	17.4305	0.07955	0.13661	0.31995	−0.64414	−1.28323
n-Butanol	18.3557	0.08322	0.13428	0.32770	−0.79278	−0.80760
n-Pentanol	22.4304	0.09939	0.13909	0.29390	−0.71205	−0.82535
n-Hexanol	27.8596	0.11829	0.15142	0.26146	−0.79141	−0.45150
n-Octanol	39.6884	0.15281	0.19141	0.23462	−0.76484	−0.42320

Eq. 11 for the pure compounds investigated in this study are listed in Table 2.

In this work, the performance of Eq. 11 is compared with the results yielded by the model of Twu et al. (1995, 1996), which uses the RK EOS (Redlich and Kwong, 1949), coupled with the following temperature functionality for α

$$\alpha = T_r^{N(M-1)} e^{L(1-T_r^{NM})} \tag{12}$$

where L, M, and N are adjustable parameters given for the appropriate representation of the vapor pressure curve. Values of these parameters for some of the compounds considered in this study were reported by Twu et al. (1995, 1996). For all other compounds these parameters were optimized as part of the present study (see Table 3).

There are two principal reasons why we have chosen the RK–Twu model for comparison of our results. First, it is known that, if the parameters of Twu's temperature functionality α are properly evaluated, Eq. 12 does not generate numerical pitfalls characteristic of other functionalities. For this reason Twu's temperature functionality α was recently implemented into a new group-contribution EOS model by Ahlers and Gmehling (2001, 2002a,b). The second reason is that the RK–Twu model was implemented by Twu et al. (1996) for the computation of data in hydrogen–hydrocarbon systems, which are particularly important for the present study. The results are presented below.

Table 3. Values of Parameters in Eq. 12

Compound	L	M	N
Nitrogen	0.10804	0.91080	3.16937
Carbon dioxide	0.18001	0.85757	2.86910
Methanol	0.53895	0.87743	2.38979
Ethanol	2.31568	2.38753	0.34386
2-Propanol	2.36562	1.76716	0.40831
n-Propanol	2.73503	1.67639	0.32391
2-Butanol	2.48397	0.49652	0.93370
n-Butanol	2.38719	0.94529	0.51923
n-Pentanol	0.54218	0.70415	1.82442
n-Hexanol	0.16765	0.75362	3.34591
n-Octanol	0.33008	0.73157	2.51880

Results and Discussion

Two factors play a major role in definition of the configuration of mixtures phase diagrams: the critical constants and the polarity of compounds. Thus, in the absence of polarity, the phase boundaries in mixtures are mainly established by the values of pure compound critical constants. Although most engineering equations of state yield exact values of critical temperatures and pressures, their ability to predict the phase diagram of nonpolar mixtures without binary parameters is usually poor, mostly because they tend to overestimate the LLE range and the CPM. On the other hand, because Eq. 11 improves the balance between VLE and LLE, this model is expected to yield better predictions for:

(1) *binary data of nonpolar systems*—without adjustment of any binary parameters, irrespective of the degree of asymmetry created by the difference between the pure compound critical constants.

(2) *binary data of polar systems*—with adjustment of one single pair of binary parameters for a complete homologous series, again irrespective of the asymmetry of particular systems.

To test the veracity of these statements, we have chosen five industrially important homologous series that constitute more that 40 binary systems. The large amount of data included here forces us to emphasize the representation of critical data that characterize phase behavior for the systems under consideration.

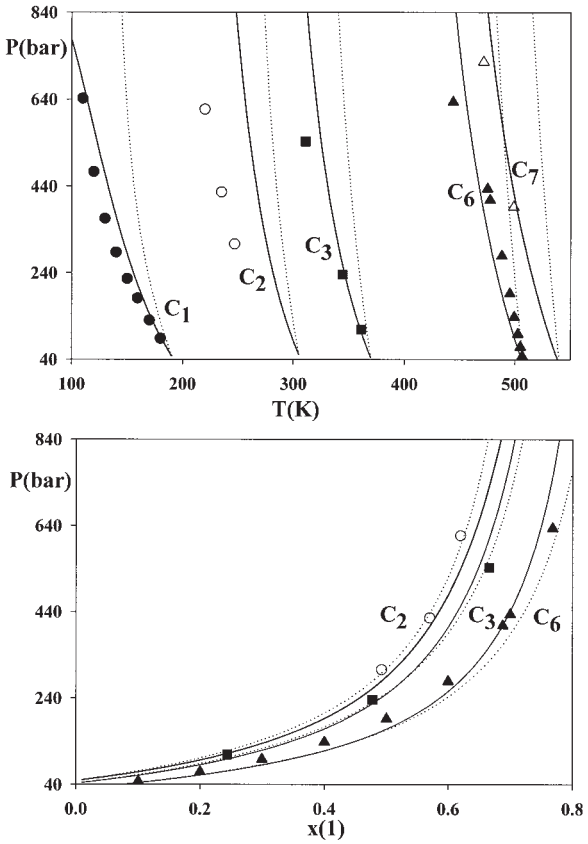

Figure 4. Critical data of hydrogen(1)–*n*-alkanes(2) predicted by the RK–Twu EOS and Eq. 11 without binary adjustable parameters.

Solid lines: data predicted by Eq. 11; dotted lines: data predicted by the RK–Twu EOS; ●: $H_2(1)$–$CH_4(2)$: experimental data of Tsang et al. (1980); ○: $H_2(1)$–$C_2H_6(2)$: experimental data of Heintz et al. (1983); ■: $H_2(1)$–n-$C_3H_8(2)$: experimental data of Buriss et al. (1953); ▲: $H_2(1)$–n-$C_6H_{14}(2)$: experimental data of Nichols et al. (1957); △: $H_2(1)$–n-$C_7H_{16}(2)$: experimental data of Peter and Reinhartz (1960).

The series we consider first is hydrogen–*n*-alkanes. Hydrogen is one of the most important gases in refinery industries. Although simulation of the data for hydrogen–*n*-alkanes is particularly necessary for the design of hydrocracking and other processes, existing models fail to describe them without introducing unusually large values of binary adjustable parameters and implementing strong temperature dependencies (Twu et al., 1996). Results depicted in Figure 4 compare the predictions of the RK–Twu model with those obtained with Eq. 11 without using any binary parameters. The accurate predictions obtained with Eq. 11 are a clear indication of the robustness of this equation. The only significant deviation from experimental data is observed in the *P–T* projection of the H_2–C_2H_6 system. However, even for this system, the results in *P–x* projection are rather accurate.

We note that hydrogen's pure compound parameters of RK–Twu EOS were precisely evaluated for a better description of the very asymmetric mixtures of hydrogen with hydrocarbons, which exhibit phase equilibria far beyond the critical temperature of hydrogen (Twu et al., 1996). As shown in Figure 4, with these pure compound hydrogen parameters the RK–Twu model is able to predict accurate results only in *P–x* projection, although the results of RK–Twu EOS in the *P–T* projection are rather poor. The importance of an accurate prediction of critical data in the *P–T* projection is illustrated in Figure 5. It can be seen that, in contrast to Eq. 11, which yields a reliable prediction of VLE in the hydrogen–propane system, the RK–Twu EOS fails to describe the data. For very asymmetric systems, such as hydrogen–*n*-alkanes, the proper description of LLE is a determinant factor for the description of other phase-equilibria behavior. Thus, the fact that the RK–Twu EOS overpredicts the data can be explained by the general tendency of van der Waals–type EOSs to overestimate the LLE range. To obtain a good fit with the RK–Twu EOS to the data in the *P–T* projection, it is necessary to use negative values of k_{12}. If this done, however, it will render negative the accurate results yielded by the model in the *P–x* projection. In other words, the introduction of binary parameters into the RK–Twu EOS fails to provide a simultaneous description of different properties. Adjustable parameters can be used only for the particular fit of the selected data. In contrast, the robust structure of Eq. 11 helps to properly predict different properties of such complex systems as hydrogen–*n*-alkanes without the introduction of binary parameters.

Similar results are obtained for two models under considerations for the asymmetric nitrogen–*n*-alkanes series. Proper description of these data is necessary for modeling important processes such as injection of nitrogen in the enhanced oil recovery. Figure 6 shows that, without binary parameters, the RK–Twu EOS fails to predict the data in both *P–x* and *P–T* projections. Moreover, the overestimation is now much more significant. In contrast, Eq. 11 yields very accurate predictions in both projections, confirming the advantages of this model.

The next series considered is methane–*n*-alkanes. Figure 7 presents the results for light *n*-alkanes up to *n*-decane and Figure 8 depicts the results for heavier *n*-alkanes. Once more, the predictions of the RKS-Twu EOS are inaccurate. In particular, the model fails to predict a continuous critical line for the methane–*n*-pentane system, which we believe is explained by

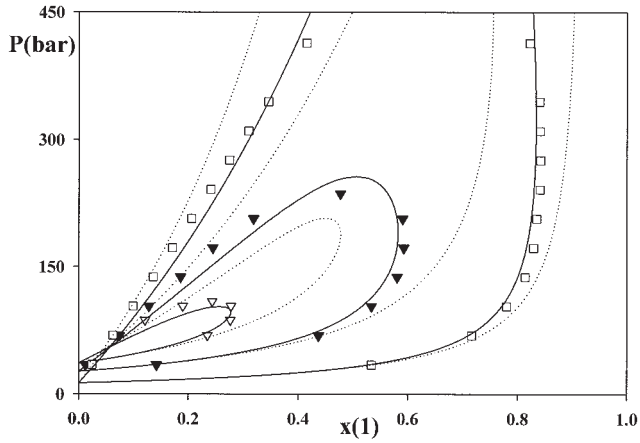

Figure 5. VLE data of hydrogen(1)–propane(2) predicted by the RK–Twu EOS and Eq. 11 without binary adjustable parameters.

Solid lines: data predicted by Eq. 11; dotted lines: data predicted by the RK–Twu EOS; experimental data of Burriss et al. (1953): ▽: 360.93 K; ▼: 344.26 K; □: 310.93 K.

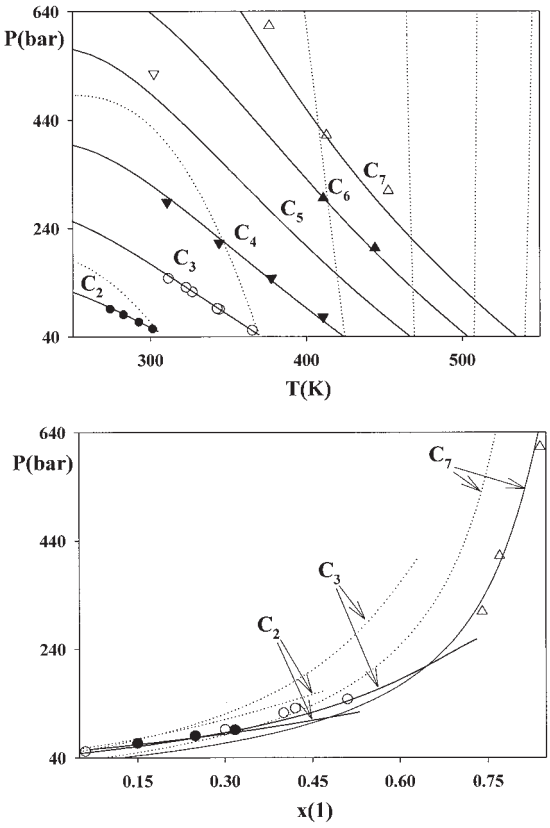

Figure 6. Critical data of nitrogen(1)–*n*-alkanes(2) predicted by the RK–Twu EOS and Eq. 11 without binary adjustable parameters.

Solid lines: data predicted by Eq. 11; dotted lines: data predicted by the RK–Twu EOS; ●: $N_2(1)$–$C_2H_6(2)$: experimental data of Eakin et al. (1955); ○: $N_2(1)$–$C_3H_8(2)$: experimental data of Roof and Baron (1967) and Schindler et al. (1966); ▼: $N_2(1)$–*n*-$C_4H_{10}(2)$: experimental data of Roberts and McKetta (1961) and Lehigh and McKetta (1961); ▽: $N_2(1)$–*n*-$C_5H_{12}(2)$: experimental data of Wisotzki and Schneider (1985); ▲: $N_2(1)$–*n*-$C_6H_{14}(2)$: experimental data of Poston and McKetta. (1966b); △: $N_2(1)$–*n*-$C_7H_{16}(2)$: experimental data of Peter and Eicke (1970).

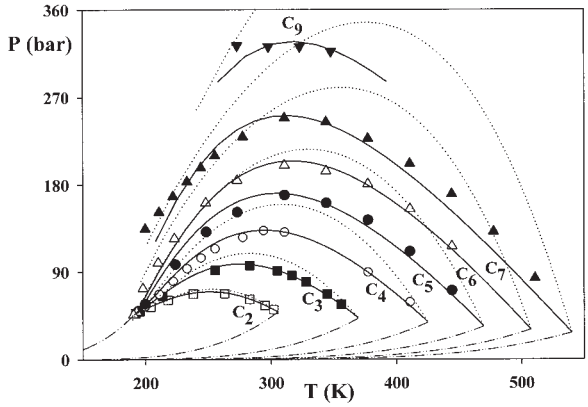

Figure 7. Critical data of methane(1)–*n*-alkanes(2) predicted by the RK–Twu EOS and Eq. 11 without binary adjustable parameters.

Solid lines: data predicted by Eq. 11; dotted lines: data predicted by the RK–Twu EOS; dot–dot–dashed lines: vapor pressure lines of pure compounds; □: $CH_4(1)$–$C_2H_6(2)$: experimental data of Bloomer et al. (1953); ■: $CH_4(1)$–$C_3H_8(2)$: experimental data of Price and Kobayashi (1959), Roof and Baron (1967), and Wichterle and Kobayashi (1972); ○: CH_4 (1)–*n*-$C_4H_{10}(2)$: experimental data of Roberts et al. (1962) and Elliot et al. (1974); ●: $CH_4(1)$–*n*-$C_5H_{12}(2)$: experimental data of Chen et al. (1978) and Sage et al. (1942); △: $CH_4(1)$–*n*-$C_6H_{14}(2)$: experimental data of Poston and McKetta (1966a) and Lin et al. (1977); ▲: $CH_4(1)$–*n*-$C_7H_{16}(2)$: experimental data of Reamer et al. (1956) and Chang et al. (1966); ▼: $CH_4(1)$–*n*-$C_9H_{20}(2)$: experimental data of Shipman and Kohn (1966).

the fact that it overestimates the range of LLE. Notably the substantial overprediction of CPMs generated by the RK–Twu EOS corresponds with its significant overestimation of the maximum pressure of the Joule–Thomson inversion curve shown in Figure 2. In addition, the deviations between the data and the results obtained with the RK–Twu EOS increase with the increasing asymmetry of the systems. This fact hinders the potential of this model to describe a complete homologous series without using binary parameters or even using a single pair of binary parameters, and requires fitting parameters for each particular system. As observed before, this behavior is typical of van der Waals–type models.

In contrast, as shown in Figures 7 and 8, the results predicted by Eq. 11 are very accurate, starting from relatively symmetric systems and up to extremely asymmetric ones, such as methane–*n*-eicosane. Such an accurate description of the data—which to the best of our knowledge cannot be achieved by any other existing EOS model—confirms our assumption that a model that gives the right balance between VLE and LLE can also predict binary nonpolar data without binary parameters, regardless of the degree of asymmetry of the molecules forming the system.

Accurate description of data in polar systems, on the other hand, requires the introduction of binary parameters. These parameters need to be evaluated using experimental data to

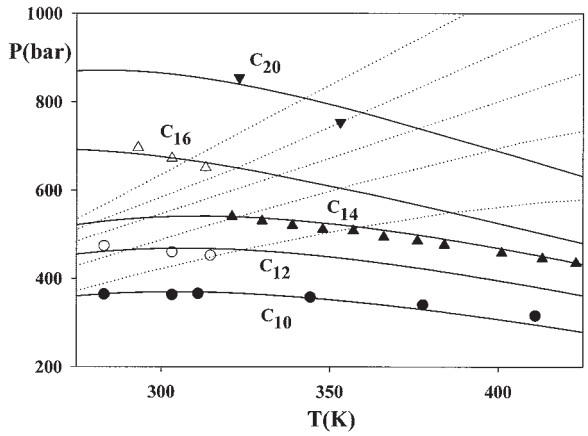

Figure 8. Critical data of methane(1)–heavy *n*-alkanes(2) predicted by the RK–Twu EOS and Eq. 11 without binary adjustable parameters.

Solid lines: data predicted by Eq. 11; dotted lines: data predicted by the RK–Twu EOS; ●: $CH_4(1)$–*n*-$C_{10}H_{22}(2)$: estimated from the data of Reamer et al. (1942) and Rijkers et al. (1992a); ○: $CH_4(1)$–*n*-$C_{12}H_{26}(2)$: estimated from the data of Rijkers et al. (1992b); ▲: $CH_4(1)$–*n*-$C_{14}H_{30}(2)$: estimated from the data of De Leeuw (1992); △: $CH_4(1)$–*n*-$C_{16}H_{34}(2)$: estimated from the data of Rijkers et al. (1993); ▼: $CH_4(1)$–*n*-$C_{20}H_{42}(2)$: estimated from the data of Ziegler et al. (1995).

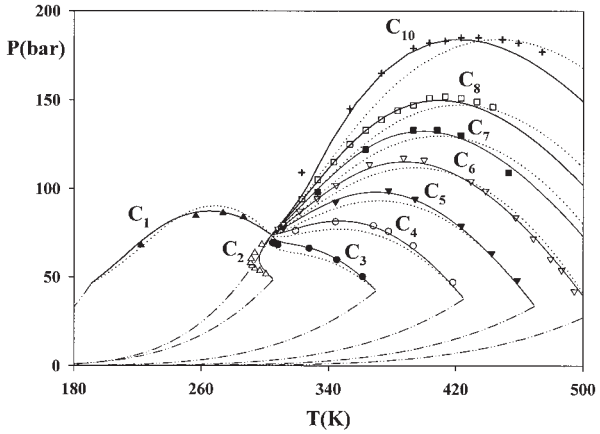

Figure 9. Critical data of carbon dioxide(1)–*n*-alkanes(2) yielded by the RK–Twu EOS (k_{12} = 0.073, l_{12} = −0.06) and Eq. 11 (k_{12} = 0.073, l_{12} = 0.02).

Solid lines: data yielded by the Eq. 11; dotted lines: data yielded by the RK–Twu EOS; dot–dot–dashed lines: vapor pressure lines of pure compounds; ▲: CH_4(1)–*n*-CO_2(2): experimental data of Donnelly and Katz (1954); △: CO_2(1)–*n*-C_2H_6(2): experimental data of Horstmann et al. (2000); ●: CO_2(1)–*n*-C_3H_8(2): experimental data of Roof and Baron (1967); ○: CO_2(1)–*n*-C_4H_{10}(2): experimental data of Hsu et al. (1985) and Leu and Robinson (1987); ▼: CO_2(1)–*n*-C_5H_{12}(2): experimental data of Cheng et al. (1989); ▽: CO_2(1)–*n*-C_6H_{14}(2): experimental data of Ziegler et al. (1995); ■: CO_2(1)–*n*-C_7H_{16}(2): experimental data of Chester and Haynes (1997); □: CO_2(1)–*n*-C_8H_{18}(2): experimental data of Ziegler et al. (1995); ✚: CO_2(1)–*n*-$C_{10}H_{22}$(2): experimental data of Chester and Haynes (1997).

include the effect that polarity exerts on phase boundaries in mixtures. However, similarly to the case of nonpolar systems, the binary parameters should not be affected by the degree of molecular asymmetry of the system. Thus, it should be possible to use the values of binary parameters obtained from a single system of a series for prediction of data for other systems of the same series. In other words, it should be possible to keep the predictive character of the EOS model.

Figure 9 compares the results obtained with the two models under consideration for the carbon dioxide–*n*-alkanes series. Data for these systems are also important for industry. The binary parameters were evaluated by simultaneously fitting the CPM and the upper critical endpoint for the CO_2–*n*-$C_{10}H_{22}$ system. Thus, both models were forced to generate the right balance between VLE and LLE for the system used to adjust the binary parameters. As shown in Figure 9, this practice substantially improves the performance of the RK–Twu EOS because the CPM calculated by this model is then fixed at the experimental value. However, the RK–Twu EOS then underestimates the data at temperatures below the CPM. Clearly, the RK–Twu EOS will require temperature-dependent k_{12} to yield accurate description of data. In addition, the poor extrapolation ability of this model is also shown by the fact that it underpredicts the data of lighter homologues. Figure 9 demonstrates clear advantages of Eq. 11, which is not only able to generate reasonable correlation of data in the CO_2–*n*-$C_{10}H_{22}$ system, but also yields very accurate predictions for the lighter homologues.

The advantage of Eq. 11 becomes more evident considering the results for another very important series: carbon dioxide–alkanols. The binary parameters have been adjusted from simultaneous correlation of the CPM and the upper critical endpoint of the CO_2–2-C_4H_9OH system, which has been the subject of intense experimental investigation (Silva-Oliver and Galicia-Luna, 2001; Stevens et al., 1997). The binary parameters so obtained have been used for predicting data of mixtures of CO_2 with both secondary and *n*-alkanol homologues. Figure 10a shows the low extrapolation ability of the RK–Twu EOS with binary parameters evaluated as described above. It can be seen that this model is unable to generate a satisfactory picture of the phase behavior. In particular, the LLE critical lines from the second and up to sixth homologues almost co-include, a behavior that obviously cannot occur in any real series. In addition, for the Type I carbon dioxide–methanol system, the model predicts a wide range of absolute liquid–liquid immis-

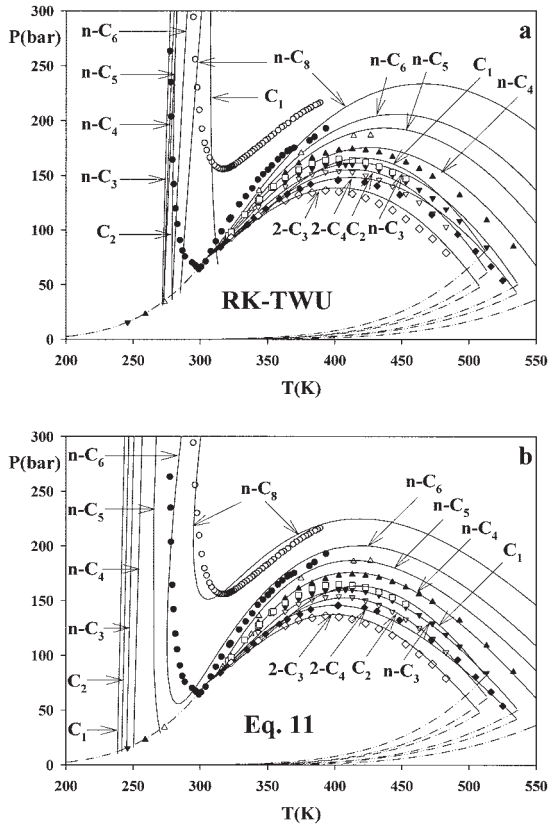

Figure 10. Critical data of carbon dioxide(1)–alkanols(2) yielded by the (a) RK–Twu EOS (k_{12} = 0.02, l_{12} = −0.10) and (b) Eq. 11 (k_{12} = 0.06, l_{12} = −0.22).

Solid lines: calculated data; dot–dot–dashed lines: vapor pressure lines of pure compounds; □: CO_2(1)–CH_3OH(2): experimental data of Ziegler et al. (1995); ▽: CO_2(1)–C_2H_5OH(2): experimental data of Ziegler et al. (1995); ◇: CO_2(1)–2-C_3H_7OH(2): experimental data of Ziegler et al. (1995); ▼: CO_2(1)–*n*-C_3H_7OH(2): experimental data of Ziegler et al. (1995) and Lam et al. (1990); ◆: CO_2(1)–2-C_4H_9OH(2): experimental data of Stevens et al. (1997) and Silva-Oliver and Galicia-Luna (2001); ▲: CO_2(1)–*n*-C_4H_9OH(2): experimental data of Ziegler et al. (1995) and Lam et al. (1990); △: CO_2(1)–*n*-$C_5H_{11}OH$(2): experimental data of Silva-Oliver et al. (2002) and Raeissi et al. (1998); ●: CO_2(1)–*n*-$C_6H_{13}OH$(2): experimental data of Scheidgen (1997); ○: CO_2(1)–*n*-$C_8H_{17}OH$(2): experimental data of Scheidgen (1997).

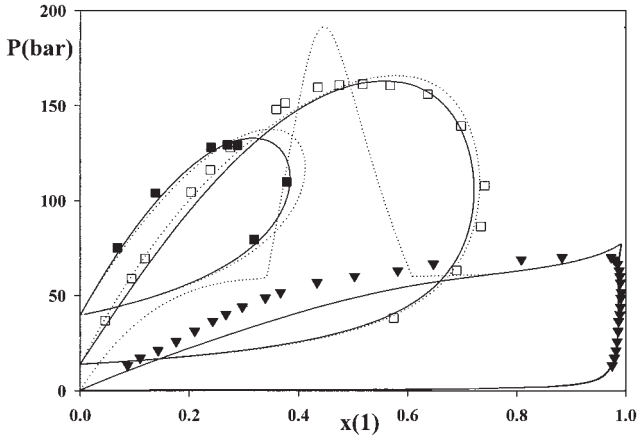

Figure 11. VLE data of carbon dioxide(1)–methanol(2) yielded by the RK–Twu EOS ($k_{12} = 0.02$, $l_{12} = -0.10$) and Eq. 11 ($k_{12} = 0.06$, $l_{12} = -0.22$).

Solid lines: data predicted by Eq. 11; dotted lines: data predicted by the RK–Twu EOS. Experimental data of Brunner et al. (1987): ■: 473.15 K; □: 423.15 K. Experimental data of Chang et al. (1998): ▼: 308.15 K.

cibility that even exceeds the critical temperature of pure carbon dioxide.

Figure 11 depicts the effect of this result on a description of phase boundaries. Whereas in the high-temperature range both models are able to satisfactorily describe the data, the RK–Twu EOS generates completely erroneous phase behavior at low temperatures. This unsatisfactory result is typical of van der Waals–like EOSs (Polishuk et al., 2001). Similarly to the results presented for the other series, the RK–Twu EOS again underestimates the VLE data at temperatures below the CPM and this inaccuracy increases with the increasing asymmetry of homologues. As a result, the model fails to yield a reasonable description of CO_2–n-$C_6H_{13}OH$ and CO_2–n-$C_8H_{17}OH$. Although in fact those systems exhibit Type III phase behavior, the RK–Twu EOS continues to predict Type II behavior for them. Thus, the EOS with parameters adjusted for an appropriate description of one of the homologues in the middle of the series overestimates the liquid–liquid split in the lighter members of the series and underestimates it for the heavier ones.

Figure 10b demonstrates the advantages of the novel EOS form presented by Eq. 11. It can be seen that, although the predictions of the model are not always precise, it gives a reasonable description of phase behavior across the series. In particular, in complete agreement with the experimental facts, the model predicts Type II behavior for *n*-propanol and *n*-butanol homologues, Type IV behavior for *n*-pentanol, and Type III behavior for the heavier homologues.

Figure 12 presents the liquid phase data along the three-phase liquid–liquid–vapor equilibrium curve of the carbon dioxide–*n*-hexanol system. In can be seen that, in contrast to RK–Twu, which fails to predict the liquid–liquid split in the region under consideration, Eq. 11 yields satisfactory results for both compositions and molar volumes. This is considered to be evidence of the reliability of this EOS for the representation of subcritical LLE data. Although Eq. 11 predicts a strong decrease of the LLE range with decrease of carbon number of the homologues, it still slightly overestimates this range for carbon dioxide–methanol and ethanol, for which the liquid–liquid split has not been detected above the temperature of solidification. In addition, it slightly underpredicts the LLE data for some heavier homologues. Nevertheless, considering the complexity of the systems under consideration, the same degree of accuracy could hardly be achieved by any other existing engineering model.

Conclusions

The aim of this work is to propose a novel approach for solving a major problem associated with the implementation of EOS models for predicting data in mixtures, that is, the overestimation of LLE range. The Dieterici EOS is unable to intersect the zero-pressure axis, which strongly restricts its prediction of liquid–liquid immiscibility. However, incorporated into the conventional van der Waals–like EOS, this expression just elevates pressures of the minimal isotherm, preserving their ability to reach the negative pressure range. As a result, the proposed EOS is capable of generating transitional VLE–LLE phase-behavior mechanisms at negative pressures, although their occurrence is hindered in comparison with the original van der Waals–like form. Thus, a combination of the Dietereci EOS with a van der Waals–type cohesive term presents a powerful tool for creating an appropriate balance between VLE and LLE in the phase diagram generated by EOS.

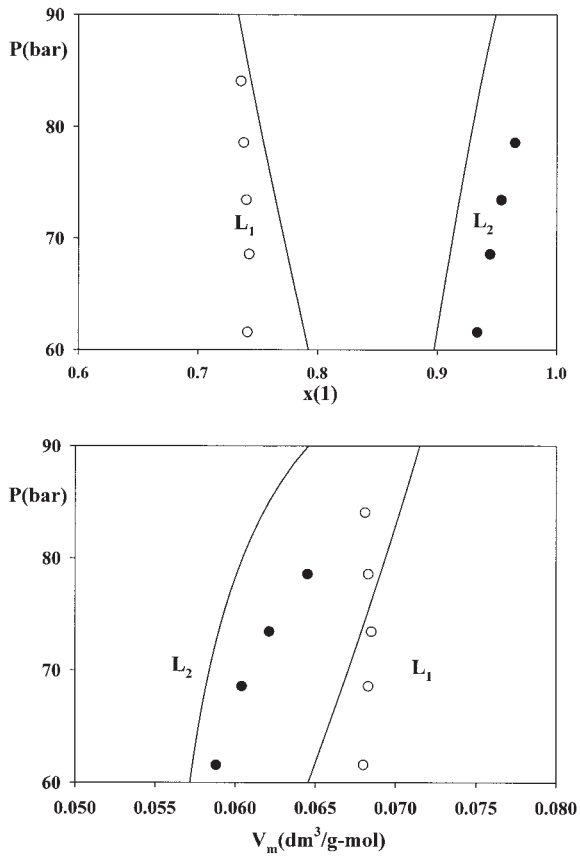

Figure 12. Three-phase liquid–liquid data yielded by Eq. 11 ($k_{12} = 0.06$, $l_{12} = -0.22$).

●, ○: Experimental data of Lam et al. (1990); solid lines: calculated data.

The importance of this tool becomes evident considering the dramatic improvement of the predictions, compared with van der Waals–type EOS models. In particular, it is demonstrated that an appropriate ratio between both van der Waals–like and Dietereci attractive terms allows:

(1) accurate presentation of the Joule–Thomson inversion curve

(2) accurate prediction of the data in nonpolar mixtures without using any binary parameters

(3) accurate prediction of the data in polar systems using a single pair of binary parameters for a complete homologous series of mixtures.

These features give the novel EOS a predictive ability that has not been achieved by any existing engineering EOS model.

In applying models for description of experimental facts it is very important to keep in mind that all regions of the thermodynamic phase space are closely interrelated. Thus, the wrong balance between LLE and VLE established by the RK–Twu EOS not only affects the region of VLE–LLE presence and its immediate surroundings at low temperatures, but also deteriorates the configuration of the entire phase diagram, including the high-temperature region.

Acknowledgments

This work was financed by Natural Sciences and Engineering Research Council (NSERC) of Canada.

Notation

a = cohesion parameter
b = covolume
c, d = volumetric parameters in Eq. 3
G^E = excess Gibbs energy
k_{12} = binary adjustable parameter of the attractive parameter
l_{12} = binary adjustable parameter of the covolume
m_1, m_2 = adjustable parameters of the α-temperature functionality (Eq. 5)
P = pressure
p = generalized EOS parameters
R = universal gas constant
T = temperature
x = mole fraction of the lighter compound
v = volume
W = weighting factor in Eq. 3

Greek letter

α = temperature functionality of the attractive parameter

Subscripts

c = critical state
r = reduced property

Abbreviations

CPM = critical pressure maximum
DCS = EOS of Dieterici–Carnahan–Starling
EOS = equation of state
LLE = liquid–liquid equilibria
RK = EOS of Redlich and Kwong (1949)
VLE = vapor–liquid equilibria

Literature Cited

Ahlers, J., and J. Gmehling, "Development of a Universal Group Contribution Equation of State. I. Prediction of Liquid Densities for Pure Compounds with a Volume Translated Peng–Robinson Equation of State," *Fluid Phase Equilib.*, **191**, 177 (2001).

Ahlers, J., and J. Gmehling, "Development of a Universal Group Contribution Equation of State. II. Prediction of Vapor–Liquid Equilibria for Asymmetric Systems," *Ind. Eng. Chem. Res.*, **41**, 3489 (2002a).

Ahlers, J., and J. Gmehling, "Development of a Universal Group Contribution Equation of State. III. Prediction of Vapor–Liquid Equilibria, Excess Enthalpies, and Activity Coefficients at Infinite Dilution with the VTPR Model," *Ind. Eng. Chem. Res.*, **41**, 5890 (2002b).

Akers, W. W., L. L. Attwell, and J. A. Robinson, "Volumetric and Phase Behavior of Nitrogen–Hydrocarbon Systems. Nitrogen–Butane System," *J. Ind. Eng. Chem.*, **46**, 2539 (1954).

Anderko, A., "Cubic and Generalized van der Waals Equations," *Equations of State for Fluids and Fluid Mixtures*, J. V. Sengers, R. F. Kayser, C. J. Peters, and H. J. White, Jr., eds., Elsevier, Amsterdam, pp. 75–126 (2002).

Bloomer, O. T., D. C. Gami, and J. D. Parent, "Physical-Chemical Properties of Methane–Ethane Mixtures," *Inst. Gas Technol. Res. Bull.*, **22**, 1 (1953).

Brunner, E., W. Hültenschmidt, and G. Schlichthärle, "Fluid Mixtures at High Pressures. IV. Isothermal Phase Equilibria in Binary Mixtures Consisting of (Methanol + Hydrogen or Nitrogen or Methane or Carbon Monoxide or Carbon Dioxide)," *J. Chem. Thermodyn.*, **19**, 273 (1987).

Bumba, J., and J. Kolafa, "Global Phase Diagrams of van der Waals–Dieterici and the BMCSL–Dieterici Equations of State," *Phys. Chem. Chem. Phys.*, **6**, 2301 (2004).

Burriss, W. L., N. T. Hsu, H. H. Reamer, and B. H. Sage, "Phase Behavior of the Hydrogen–Propane System," *J. Ind. Eng. Chem.*, **45**, 210 (1953).

Carnahan, N. F., and K. E. Starling, "Equation of State for Non-attracting Rigid Spheres," *J. Chem. Phys.*, **51**, 635 (1969).

Chang, C. J., K. L. Chiu, and C. Y. Day, "A New Apparatus for the Determination of P–x–y diagrams and Henry's Constants in High Pressure Alcohols with Critical Carbon Dioxide," *J. Supercrit. Fluids*, **12**, 223 (1998).

Chang, H. L., L. J. Hurt, and R. Kobayashi, "Vapor–Liquid Equilibria of Light Hydrocarbons at Low Temperatures and High Pressures: The Methane–*n*-Heptane System," *AIChE J.*, **12**, 1212 (1966).

Chen, R. J. J., P. S. Chappelear, and R. Kobayashi, "Dew-Point Loci for Methane–*n*-Pentane Binary System," *J. Chem. Eng. Data*, **19**, 58 (1978).

Cheng, H., M. E. Pozo de Fernandez, J. A. Zollweg, and W. B. Streett, "Vapor–Liquid Equilibrium in the System Carbon Dioxide + *n*-Pentane from 252 to 458 K at Pressures to 10 MPa," *J. Chem. Eng. Data*, **34**, 319 (1989).

Chester, T. L., and B. S. Haynes, "Estimation of Pressure–Temperature Critical Loci of CO_2 Binary Mixtures with Methyl-*tert*-Butyl Ether, Ethyl Acetate, Methyl-Ethyl Ketone, Dioxane and Decane," *J. Supercrit. Fluids*, **11**, 15 (1997).

De Leeuw, V. V., T. W. De Loos, H. A. Kooijman, and J. De Swaan Arons, "The Experimental Determination and Modeling of VLE for Binary Subsystems of the Quaternary System Nitrogen + Methane + Butane + Tetradecane up to 1000 bar and 440 K," *Fluid Phase Equilib.*, **73**, 285 (1992).

Donnelly, H. G., and D. L. Katz, "Phase Equilibria in the Carbon Dioxide–Methane System," *J. Ind. Eng. Chem.*, **46**, 511 (1954).

Eakin, B. E., R. T. Ellington, and D. C. Gami, "Physical-Chemical Properties of Ethane–Nitrogen Mixtures," *Inst. Gas Technol. Res. Bull.*, **26**, 1 (1955).

Elliot, D. G., R. J. J. Chen, P. S. Chappelear, and R. Kobayashi, "Vapor–Liquid Equilibrium of Methane–Butane System at Low Temperatures and High Pressures," *J. Chem. Eng. Data*, **19**, 71 (1974).

Heintz, A., and W. B. Streett, "Phase Equilibriums in the Hydrogen/Ethylene System at Temperatures from 114.1 to 247.1 K and Pressures to 600 MPa," *Ber. Bunsen-Ges. Phys. Chem.*, **87**, 298 (1983).

Horstmann, S. K., K. Fischer, J. Gmehling, and P. Kolar, "Experimental Determination of the Critical Line for (Carbon Dioxide + Ethane) and Calculation of Various Thermodynamic Properties for (Carbon Dioxide + *n*-Alkane) Using the PSRK Model," *J. Chem. Thermodyn.*, **32**, 451 (2000).

Hsu, J. J. C., N. Nagarajan, and R. L. Robinson, Jr., "Equilibrium Phase Compositions, Phase Densities, and Interfacial Tensions for Carbon Dioxide + Hydrocarbon Systems. 1. Carbon Dioxide + *n*-Butane," *J. Chem. Eng. Data*, **30**, 485 (1985).

Huron, M. J., and J. Vidal, "New Mixing Rules in Simple Equations of

State for Representing Vapour–Liquid Equilibria of Strongly Non-ideal Mixtures," *Fluid Phase Equilib.*, **3**, 255 (1979).
Lam, D. H., A. Jangkamolkulchai, and K. D. Luks, "Liquid–Liquid–Vapor Phase Equilibrium Behavior of Certain Binary Carbon Dioxide + *n*-Alkanol Mixtures," *Fluid Phase Equilib.*, **60**, 131 (1990).
Leu, A. D., and D. B. Robinson, "Equilibrium Phase Properties of the *n*-Butane–Carbon Dioxide and Isobutene–Carbon Dioxide Binary Systems," *J. Chem. Eng. Data*, **32**, 444 (1987).
Lin, Y. N., R. J. J. Chen, P. S. Chappelear, and R. Kobayashi, "Vapor–Liquid Equilibrium of Methane–*n*-Hexane System at Low Temperature," *J. Chem. Eng. Data*, **22**, 402 (1977).
Nichols, W. B., H. H. Reamer, and B. H. Sage, "Volumetric and Phase Behavior in the Hydrogen–Hexane System," *AIChE J.*, **3**, 262 (1957).
Peng, D. Y., and D. B. Robinson, "A New Two-Constant Equation of State," *Ind. Eng. Chem. Fundam.*, **15**, 59 (1976).
Perry, R. H., D. W. Green, and J. O. Maloney, *Perry's Chemical Engineers' Handbook*, 7th Edition, McGraw-Hill, New York (1999).
Peter, S., and H. F. Eicke, "Phase Equilibrium in the Systems Nitrogen–*n*-Heptane, Nitrogen-2,2,4-trimethylpentane, and Nitrogen–Methylcyclohexane at Higher Pressures and Temperatures," *Ber. Bunsen-Ges. Phys. Chem.*, **74**, 190 (1970).
Peter, S., and K. Reinhartz, "Phase Equilibrium in the Systems H_2–*n*-Heptane, H_2–Methylcyclohexane, and H_2–2,2,4-Trimethylpentane at Elevated Pressures and Temperatures," *Z. Phys. Chem.*, **24**, 103 (1960).
Polishuk, I., R. González, J. H. Vera, and H. Segura, "Phase Behavior of Dieterici Fluids," *Phys. Chem. Chem. Phys.*, **6**, 5189 (2005).
Polishuk, I., R. P. Stateva, J. Wisniak, and H. Segura, "Prediction of High-Pressure Phase Equilibria Using Cubic EOS: What Can Be Learned?," *Can. J. Chem. Eng.*, **80**, 927 (2002).
Polishuk, I., J. Wisniak, and H. Segura, "Prediction of the Critical Locus in Binary Mixtures Using Equation of State. I. Cubic Equations of State, Classical Mixing Rules, Mixtures of Methane–Alkanes," *Fluid Phase Equilib.*, **164**, 13 (1999).
Polishuk, I., J. Wisniak, and H. Segura, "Simultaneous Prediction of the Critical and Sub-critical Phase Behavior in Mixtures Using Equations of State. I. Carbon Dioxide–Alkanols. *Chem. Eng. Sci.*, **56**, 6485 (2001).
Polishuk, I., J. Wisniak, and H. Segura, "Simultaneous Prediction of the Critical and Sub-critical Phase Behavior in Mixtures Using Equations of State. II. Carbon Dioxide–Heavy *n*-Alkanes," *Chem. Eng. Sci.*, **58**, 2529 (2003).
Polishuk, I., J. Wisniak, H. Segura, L. V. Yelash, and T. Kraska, "Prediction of the Critical Locus in Binary Mixtures Using Equation of State. II. Investigation of van der Waals–Type and Carnahan–Starling-Type Equations of State, " *Fluid Phase Equilib.*, **172**, 1 (2000).
Poston, R. S., and J. J. McKetta, "Vapor–Liquid Equilibrium in the Methane–*n*-Hexane System," *J. Chem. Eng. Data*, **11**, 362 (1966a).
Poston, R. S., and J. J. McKetta, "Vapor–Liquid Equilibrium in the *n*-Hexane–Nitrogen System," *J. Chem. Eng. Data*, **11**, 364 (1966b).
Price, A. R., and R. Kobayashi, "Low-Temperature Vapor–Liquid Equilibrium in Light Hydrocarbon Mixtures: Methane–Ethane–Propane System," *J. Chem. Eng. Data*, **4**, 40 (1959).
Raeissi, S., K. Gauter, and C. J. Peters, "Fluid Multiphase Behavior in Quasi-Binary Mixtures of Carbon Dioxide and Certain 1-Alkanols," *Fluid Phase Equilib.*, **147**, 239 (1998).
Reamer, H. H., R. H. Olds, B. H. Sage, and W. N. Lacey, "Phase Equilibria in Hydrocarbon Systems. Methane–*n*-Decane System," *J. Ind. Eng. Chem.*, **34**, 1526 (1942).
Reamer, H. H., B. H. Sage, and W. N. Lacey, "Volumetric and Phase Behavior of the Methane–*n*-Heptane System," *Chem. Eng. Data Ser.*, **1**, 29 (1956).
Redlich, O., and J. N. S. Kwong, "On the Thermodynamics of Solutions: V. An Equation of State: Fugacities of Gaseous Solutions," *Chem. Rev.*, **44**, 233 (1949).
Rijkers, M. P. W. M., V. B. Maduro, C. J. Peters, and J. De Swaan Arons, "Measurements on the Phase Behavior of Binary Mixtures for Modeling the Condensation Behavior of Natural Gas. Part II. The System Methane + Dodecane," *Fluid Phase Equilib.*, **72**, 309 (1992b).
Rijkers, M. P. W. M., M. Malais, C. J. Peters, and J. De Swaan Arons, "Measurements on the Phase Behavior of Binary Hydrocarbon Mixtures for Modeling the Condensation Behavior of Natural Gas. Part I. The System Methane–Decane," *Fluid Phase Equilib.*, **71**, 143 (1992a).
Rijkers, M. P. W. M., C. J. Peters, and J. De Swaan Arons, "Measurements on the Phase Behavior of Binary Mixtures for Modeling the Condensation Behavior of Natural Gas. Part III. The System Methane + Hexadecane," *Fluid Phase Equilib.*, **85**, 335 (1993).
Roberts, L. R., R. H. Wang, A. Azarnoosh, and J. J. McKetta, "Methane–Butane System in the Two-Phase Region," *J. Chem. Eng. Data*, **7**, 484 (1962).
Roof, J. G., and J. D. Baron, "Critical Loci of Binary Mixtures of Propane with Methane, Carbon Dioxide, and Nitrogen," *J. Chem. Eng. Data*, **12**, 292 (1967).
Sadus, R. J., "Equation of State for Fluids: The Dieterici Approach Revisited," *J. Chem. Phys.*, **115**, 1460 (2001). [*Erratum.* **115**, 5913 (2002a)].
Sadus, R. J., "The Dieterici Alternative to the van der Waals Approach for Equations of State: Second Virial Coefficient," *Phys. Chem. Chem. Phys.*, **4**, 919 (2002b).
Sadus, R. J., "New Dieterici-Type Equation of State for Fluid Phase Equilibria," *Fluid Phase Equilib.*, **212**, 31 (2003).
Sage, B. H., H. H. Reamer, R. H. Olds, and W. N. Lacey, "Phase Equilibria in Hydrocarbon Systems. Volumetric and Phase Behavior of Methane–Pentane System," *Ind. Eng. Chem.*, **34**, 1108 (1942).
Scheidgen, A., *Fluid Phase Equilibria in Binary and Ternary Mixtures of Carbon Dioxide with Low-Volatile Organic Substances up to 100 MPa* (in German), Ph.D. Dissertation, Ruhr-Universität Bochum, Bochum, Germany (1997).
Schindler, D. L., G. W. Swift, and F. Kurata, "More Low-Temperature Vapor–Liquid Design Data," *Hydrocarb. Process. Petrol. Refiner.*, **45**, 205 (1966).
Shipman, L. M., and J. P. Kohn, "Heterogeneous Phase and Volumetric Equilibrium in the Methane–*n*-Nonane System," *J. Chem. Eng. Data*, **11**, 176 (1966).
Silva-Oliver, G., and L. A. Galicia-Luna, "Vapor–Liquid Equilibria Near Critical Point and Critical Points for the CO_2 + 1-Butanol and CO_2 + 2-Butanol Systems at Temperatures from 324 to 432 K," *Fluid Phase Equilib.*, **182**, 145 (2001).
Silva-Oliver, G., L. A. Galicia-Luna, and S. I. Sandler, "Vapor–Liquid Equilibria and Critical Points for the Carbon Dioxide + 1-Pentanol and Carbon Dioxide + 2-Pentanol Systems at Temperatures from 332 to 432 K," *Fluid Phase Equilib.*, **200**, 161 (2002).
Stevens, R. M. M., J. C. van Roermund, M. D. Jager, Th. W. de Loos, and J. de Swaan Arons, "High-Pressure Vapor–Liquid Equilibria in the Systems Carbon Dioxide + 2-Butanol, + 2-Butyl Acetate, + Vinyl Acetate and Calculations with Three EOS Methods," *Fluid Phase Equilib.*, **138**, 159 (1997).
Tsang, C. Y., P. Clancy, J. C. G. Calado, and W. B. Streett, "Phase Equilibriums in the Hydrogen/Methane System at Temperatures from 92.3 to 180.0 K and Pressures to 140 MPa," *Chem. Eng. Commun.*, **6**, 365 (1980).
Twu, C. H., J. E. Coon, and J. R. Cunningham, "A New Generalized Alpha Function for a Cubic Equation of State. Part 2. Redlich–Kwong Equation," *Fluid Phase Equilib.*, **105**, 61 (1995).
Twu, C. H., J. E. Coon, A. H. Harvey, and J. R. Cunningham, "An Approach for the Application of a Cubic Equation of State to Hydrogen–Hydrocarbon Systems," *Ind. Eng. Chem. Res.*, **35**, 905 (1996).
Valderrama, J. O., "The State of the Cubic Equations of State," *Ind. Eng. Chem. Res.*, **42**, 1603 (2003).
van der Kooi, H. J., E. Floter, and Th. W. de Loos, "High-Pressure Phase Equilibria of $\{(1 - x)CH_4 + xCH_3(CH2)_{18}CH_3\}$," *J. Chem. Thermodyn.,* **27**, 847 (1995).
Wichterle, I., and R. Kobayashi, "Vapor–Liquid Equilibrium of Methane–Propane System at Low Temperatures and High Pressures," *J. Chem. Eng. Data*, **17**, 4 (1972).
Wisniak, J., and H. Avraham, "On the Joule–Thomson Effect Inversion Curve," *Thermochim. Acta*, **286**, 33 (1996).
Wisotzki, K. D., and G. M. Schneider, "Fluid Phase Equilibria of the Binary Systems Molecular Nitrogen + Ethane and Molecular Nitrogen + Pentane between 88 K and 313 K and at Pressures up to 200 MPa," *Ber. Bunsen-Ges. Phys. Chem.*, **89**, 21 (1985).
Ziegler, J. W., T. L. Chester, D. P. Innis, S. H. Page, and J. G. Dorsey, "Supercritical Fluid Flow Injection Method for Mapping Liquid–Vapor Critical Loci of Binary Mixtures Containing CO_2," *ACS Symp. Ser.*, **608**, 93 (1995).

Appendix: Fugacity Coefficients of the Dieterici–van der Waals EOS

The fugacity coefficient of a pure compound obtained from the Dieterici–van der Waals EOS takes the form

$$\ln \phi = (Z-1) - \ln Z + \left[E_i\left(-\frac{Wa}{RTv}\right) - \gamma_E - \ln\left(\frac{Wa}{RTv}\right)\right] + \left\{E_i\left(\frac{Wa}{RTb}\right) - E_i\left[\frac{Wa(v-b)}{RTbv}\right]\right\}\exp\left(-\frac{Wa}{RTb}\right) - \frac{a}{RT(v+c)} \tag{A1}$$

where $\gamma_E \approx 0.577216\cdots$ is Euler's gamma constant and $E_i(X)$ is Euler's exponential integral function, defined as

$$E_i(X) = -\int_{-X}^{\infty} \frac{e^{-t}}{t}\,dt = \gamma_E + \ln|X| + \sum_{k=1}^{\infty} \frac{X^k}{kk!} \tag{A2}$$

For a compound i in a mixture, the fugacity coefficient obtained from the Dieterici–van der Waals EOS takes the form

$$ln\ \phi_i = \left[E_i\left(-\frac{Wa}{RTv}\right) - \gamma_E - \ln\left(\frac{Wa}{RTv}\right)\right) - \frac{\bar{b}_i}{b}\left[1 - \left(\frac{v}{v-b}\right)\exp\left(-\frac{Wa}{RTv}\right)\right] + \left\{E_i\left(\frac{Wa}{RTb}\right) - E_i\left[\frac{Wa(v-b)}{RTbv}\right]\right\} \times \left[1 - \frac{(\overline{Wa_i}b - Wa\bar{b}_i)}{RTb^2}\right]\exp\left(-\frac{Wa}{RTb}\right) - \frac{\bar{a}_i + a}{RT(v+c)} + \frac{a\bar{c}_i}{RT(v+c)^2} - \ln Z \tag{A3}$$

Using Eqs. 6 and 9 of the text for $\overline{Wa}_i$ and $\bar{a}_i$, or Eqs. 6 and 10 of the text for $\bar{b}_i$, we obtain

$$\bar{p}_i = \left(\frac{\partial np}{\partial n_i}\right)_{T,nv,n_{j\neq i}} = 2\sum_{j=1}^{c} x_j p_{ij} - p \tag{A4}$$

and for $\bar{c}_i$ using Eqs. 6 and 8 of the text, we write

$$\bar{c}_i = \left(\frac{\partial nc}{\partial n_i}\right)_{T,nv,n_{j\neq i}} = c_i \tag{A5}$$

For direct calculations, Eqs. A1 and A3 can be simplified replacing Euler's integral functions by their equivalent forms given by Eq. A2.

Manuscript received July 17, 2004, and revision received Nov. 9, 2004.